JOURNAL OF THE BALKAN GEOPHYSICAL SOCIETY, Vol. 3, No 2, May 2000, p. 20-36, 13 figs.

The effect of the initial earthquake phase shift on the inversion of regional surface wave recordings for the estimation of crustal structure

Özcan Çakir, Murat Erduran and Salih Livaoğlu

Department of Geophysics, Black Sea Technical University, 61080, Trabzon, Turkey

(Received 03 December 1999; accepted 24 February 2000)

***Abstract**: The single-station surface wave inversion is a powerful tool for crustal structure exploration. High quality earthquake recordings at far-field seismic stations can be used to perform such kind of inversion. In this process, the frequency dependent phase shift that seismic waves acquire at the focal area, should be removed from the observed dispersion curves. This is often a difficult task to achieve particularly for minor earthquakes. In the present work, we attempt a numerical simulation of this problem by employing synthetic seismograms and investigate the case where no correction is made for the source phase shift before the group velocity inversion. After performing the inversion, very satisfactory results were obtained particularly for shallow depths, i.e. upper and middle crustal levels. In some cases, inversion gave poor resolution for velocities at lower crustal levels, for which a forward synthetic seismogram modeling is suggested in order to recover the missing information at those levels. The results of the present study show that synthetic modeling is necessary for modeling surface wave recordings at local and regional distances. The case of anisotropic wave propagation in the crust has also been studied with an emphasis on the false identification of anisotropy provided that no corrections are applied for the source phase shift. This erroneous anisotropy identification is caused by the Rayleigh and Love wave incompatibility and can have serious practical consequences for surface wave modeling.*

***Key words**: Source Phase Shift, Focal Mechanism, Source Time Function, Regional Earthquakes, Group Velocity Inversion, Anisotropy.*

INTRODUCTION

Surface wave recordings of regional earthquakes can be efficiently used to explore the crustal structure around a seismic station capable of recording three component ground motion. Depending on the distance at which an earthquake is observed, deep seismic velocities of the crust can be retrieved by inversion of surface wave recordings (Mindevalli and Mitchell, 1989, Mokhtar and Al-Saeed, 1994). Two-station and single-station methods are frequently used for such an analysis. There are certain advantages and disadvantages of both methods. In the two-station method, the receivers should lie on the same great circle path from the event. In this method, the seismic signal recorded at the first station is deconvolved from the one recorded at the second station so that the signal obtained is equivalent to the one that would be observed at the second station for an impulse (phase free) source at the first station. Depending on how appropriately and densely the seismic stations are placed with respect to the regional seismicity, it is possible to find some suitable propagation paths for a two-station analysis. However, there are several cases where the conditions for the application of the two-station method can not be met and where the single-station method is the only way to analyze the data. In several cases the two approaches are utilized simultaneously, depending on the available event and station path coverage (Navarro *et al*., 1997).

The initial earthquake phase shift is an important factor which has to be taken into account, particularly when considering the local (<100 km) and regional (100<X<1400 km) surface wave propagation for structural estimation with the single-station approach (Dziewonski and Hales, 1972). The initial source phase for a given azimuth is a function of the rupture mechanism, source time function and elastic parameters around the source region (Levshin *et al*., 1999, Frez and Schwab, 1976). In the case when the source phase is constant or slowly varying with frequency, the observed group velocities, which are proportional to the derivative of the total propagation phase, are not significantly affected by not taking into account the initial phase shift. The source phase shift can be

calculated for a given azimuth and frequency if the source parameters and the structure in the vicinity of the epicenter is known (Aki and Richards, 1980), and thus the phase effect can be removed from the recordings. However, in practice this is usually a difficult task because the fault plane solutions are often difficult to obtain for minor earthquakes, which are frequently used in surface wave studies. The phase function is more important for local and regional earthquakes and becomes gradually less effective at and beyond upper-mantle distances of 1400<X<3000 km (see Levshin *et al*., 1999).

In the present study, we analyze the single-station method and the effect of the initial earthquake phase shift. The impact of omitting the effect of this initial phase on group velocity inversion is discussed on the basis of some numerical calculations. We have selected three different models which are representative of some typical crustal structures. Four different focal mechanisms (strike slip, dip slip, normal and reverse oblique faulting) are also considered in the calculations. The source moment rate functions are assumed to be represented by the combination of simple triangular pulses. Synthetic seismograms, based on the reflectivity method (Müller, 1985), are calculated for each source combination given above for a shallow focal depth (10 km) event at an epicentral distance of 350 km. After applying the multiple filter technique (Hermann, 1973) to the synthetic seismograms, we obtained group velocities. The linearized least-square inversion technique is applied to the group velocities to estimate the elastic parameters for the propagation path.

It should be noted that we performed the analysis in this work for only one epicentral distance (350 km). There are two reasons for that. First, we aimed to show the effect of the source phase shift on the group velocity inversion as much as possible and that required that the epicentral distance be small, because the source effect is reduced with increasing the epicentral distance. On the other hand, the epicentral distance should not be too small if one seeks to obtain the crustal response of surface waves, because the penetration depth of surface waves increases with increasing the epicentral distance. Therefore, the choice of the 350 km for an epicentral distance is reasonable with the view to matching the two cases above. Certainly, in the case of applications for real data, the epicentral distance range of specific interest should be tested beforehand.

The proposed analysis is particularly applicable for regions with high medium-scale seismic activity observed by relatively poor station coverage, as is the case in eastern Anatolia. In regions of large crustal deformation, such as eastern Anatolia (Barka and Kadinsky-Cade, 1988), anisotropic wave propagation (Crampin and Booth, 1985, Maslova and Obolentseva, 1984, Mitchell, 1984) could be an important factor to be included in the analysis. Therefore, we considered the effect of anisotropy in our analysis and tested the efficiency of the single station surface wave method in resolving a possible crustal anisotropic structure. Finally, we present a case study of an earthquake which occurred in the middle section of north Anatolia.

SELECTED TEST MODEL STRUCTURES

The main aim of the current study is focusing on the crustal structure, hence only the shallow depths (up to 70 km) were considered. The employed test model structures are illustrated in Figures 1a-c, where the shear velocity depth distributions are shown on the left and the corresponding theoretical fundamental mode Rayleigh and Love wave dispersion curves are presented on the right side. Poisson ratio (σ) in each layer was assumed to be 0.25 and the densities (ρ) are calculated from the compressional velocities (α) using the relation $0.32\alpha+0.77$ (Ammon *et al*., 1990). The normal mode calculation is based on a work by Chen (1993). The shear velocity structure presented as Model 1 (Fig. 1a) is adapted from the work of Mindevalli and Mitchell (1989) derived for the crustal structure under eastern Anatolia. This model features an almost constant positive velocity gradient with depth, except for depths of around 15 km where velocity keeps a constant value of about 3.6 km/s. It is also noted that there is no first order velocity jump in the model such as the one observed at the Moho discontinuity, although a crustal thickness of approximately 40 km can be estimated. Dispersion curves for this model (on the right side in Figure 1a) are quite regular and it is obvious that an Airy phase for Rayleigh waves originates in the 10-20 s period range with a group velocity of about 2.8 km/s, whereas the group velocities at the 40 s period reach as high as 3.5 km/s.

The second model tested (Fig. 1b) has a rather low crustal thickness (about 20 km) and has a high positive velocity gradient. Below a depth of 20 km we have added a low velocity zone in order to test the sensitivity of the inversion technique to this depth range. Since the crustal thickness is relatively low, the group velocities quickly increase and reach the value of about 4 km/s at the 40 s period. Because of the velocity depth distribution of this model, Rayleigh waves are faster than Love waves in the period range 10-20 s.

The last selected model is shown in Figure 1c and exhibits strongly varying features with one low velocity

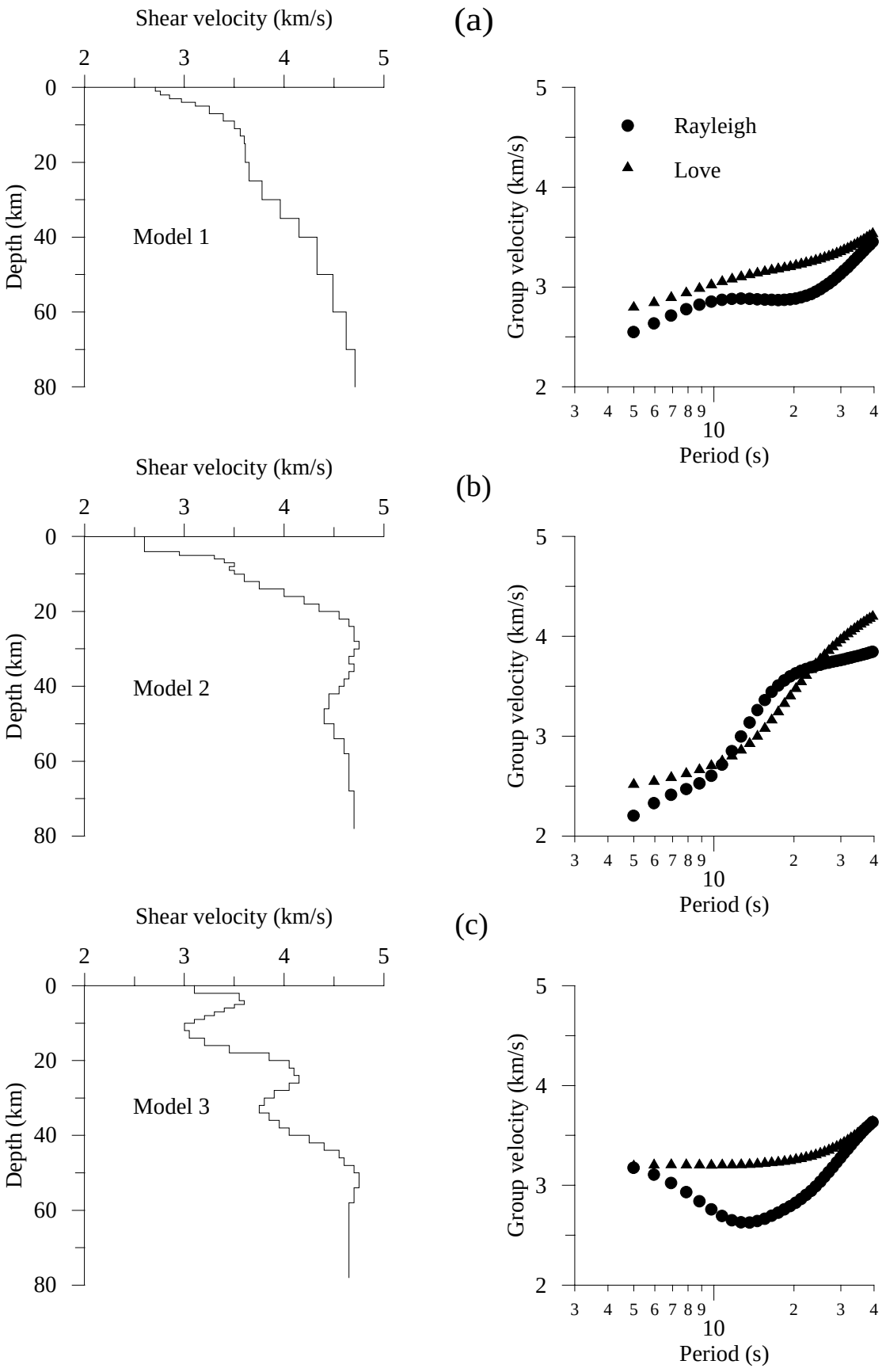

FIG. 1. Selected model structures for a single station surface wave analysis in the crust. Shear velocity depth distributions are shown on the left and the corresponding theoretical fundamental mode group velocities for Rayleigh and Love waves are shown on the right side.

zone in the upper crust and a second one in the lower crust. The crustal thickness was fixed at 50 km and the uppermost mantle velocity was set to be equal to 4.7 km/s. Here the Love waves show almost no dispersion until the 20 s period and the normal dispersion carries the Love wave fundamental mode energy at higher periods. Rayleigh waves show both normal and reverse dispersion and reach a minimum group velocity slightly below the 15 s period.

FOCAL MECHANISMS AND MOMENT RATE FUNCTIONS

The selected focal mechanisms include strike slip, dip slip, normal and reverse oblique faulting (Table 1) and cover the range most frequently observed in seismicity studies (Levshin *et al*., 1999). All the main fault planes are arranged to strike 90^{o} from the north, and the dip and slip angles are allowed to vary as shown in Table 1.

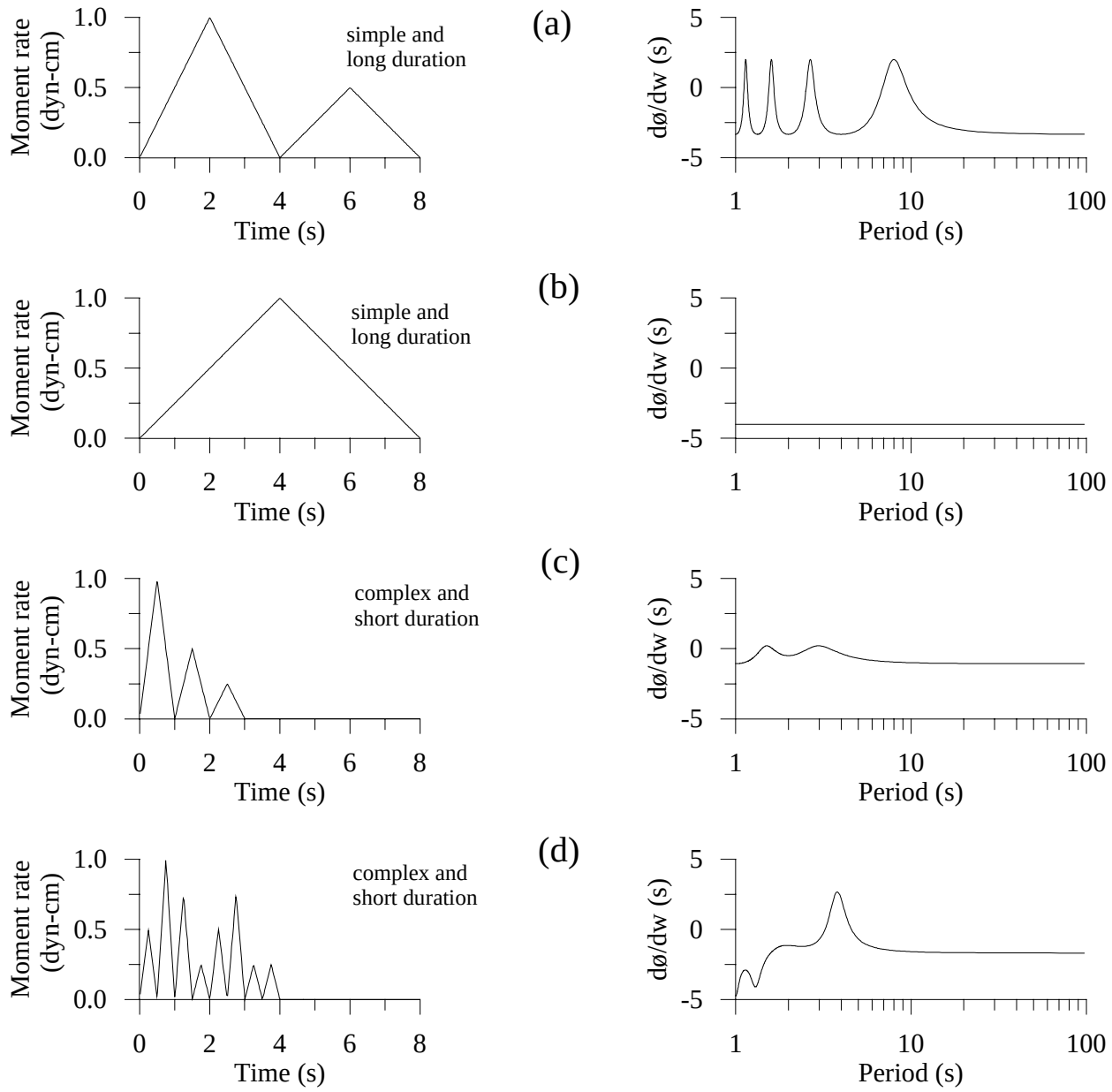

FIG. 2. Selected source time functions on the left and the corresponding phase (*ø*) derivatives with respect to the angular frequency (*w*) on the right. Phase derivative functions show phase delay and advance in seconds. The upper two functions denote simple and long duration ruptures, while the lower two represent complex and short rupture durations.

Table 1. Focal mechanism parameters utilized in the current work.

Strike/Dip/Rake

Strike-slip	Dip-slip	Normal	Oblique-reverse
90/90/180	90/90/-90	90/45/-90	90/45/45

The selected moment rate functions are illustrated in Figure 2. The rupture time history of each event is configured as either a complex or a relatively simple one and as a short or a relatively long duration. On the left side of Figure 2 we present the moment rate functions for each configuration and the corresponding time shift functions with respect to the period on the right. The source time functions in Figures 2a and 2b represent a long duration and a simple rupture event. The phase delay and advance functions on the right are produced from an angular frequency (w) derivative of the phase spectrum (ϕ) and reflect the amount of time delay or advance of each Fourier harmonic caused by the time history alone at the source. It is noted that the phase derivative functions in seconds are relatively smooth at high periods and become relatively complex at low periods. This behavior of the source time function will influence particularly the small period fundamental and higher mode surface wave modes during the multiple filter analysis of records. The second source time function is a single triangular pulse centered at 4 s and all the harmonics at the source are delayed by the same amount of 4 s (see Fig. 2b).

We have selected two other source time functions as shown in Figures 2c and 2d. These are both complex, represented by a sequence of simple triangular pulses and also a short duration. The phase derivative functions at the right are smoother compared to the first two above. In the case when the source moment rate function is an impulse, the corresponding phase derivative will be equivalent to zero and thus the phase spectrum at the source will only be a function of the type of focal mechanism and of the elastic parameters in the source region.

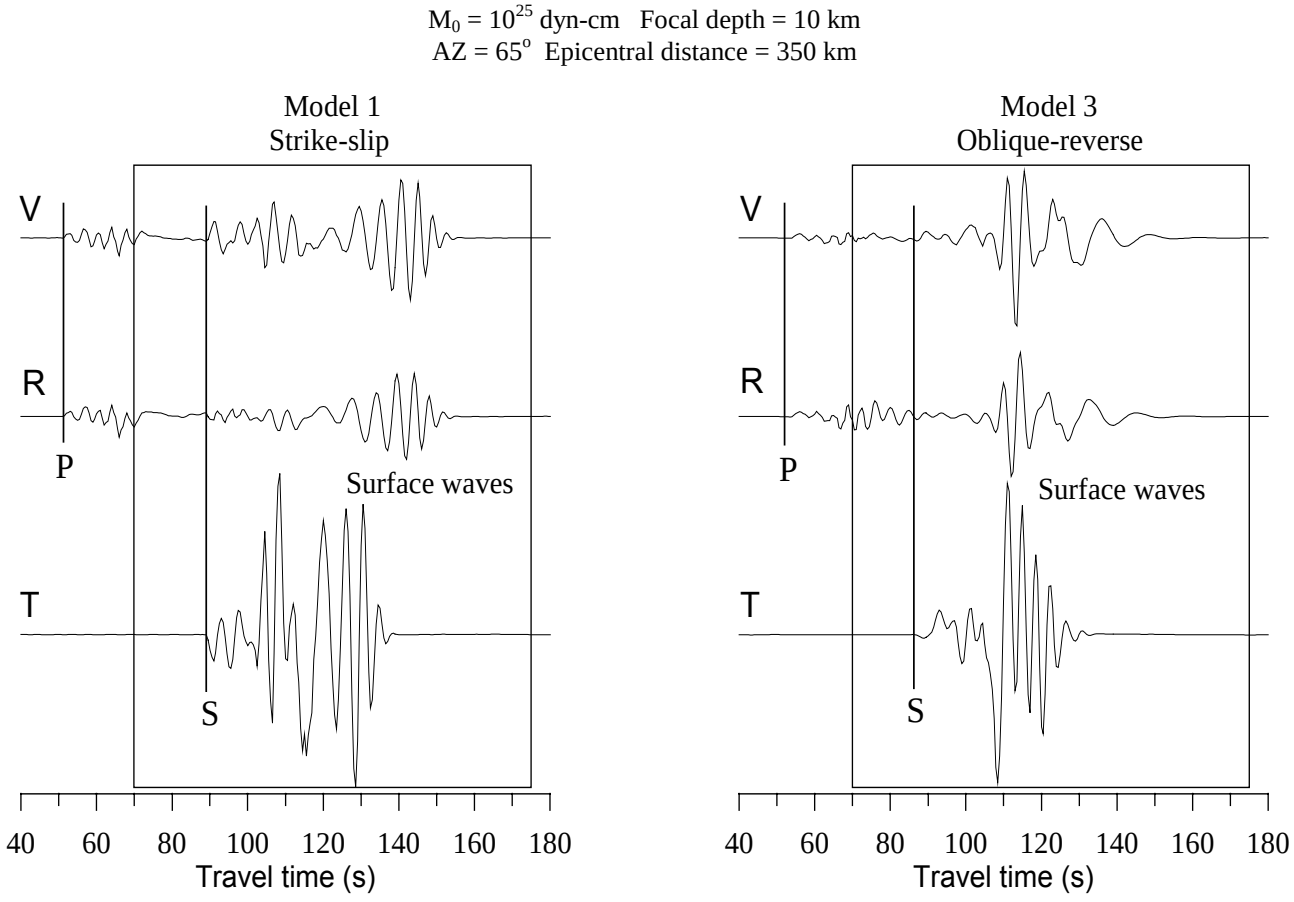

FIG. 3. Examples of two regional three-component synthetic seismograms (particle velocity). The velocity structures of Model 1 (Fig. 1a) and Model 3 (Fig. 1c) are used for source and propagation media. A source time function in Figure 3a is employed and the other source parameters used are indicated on top.

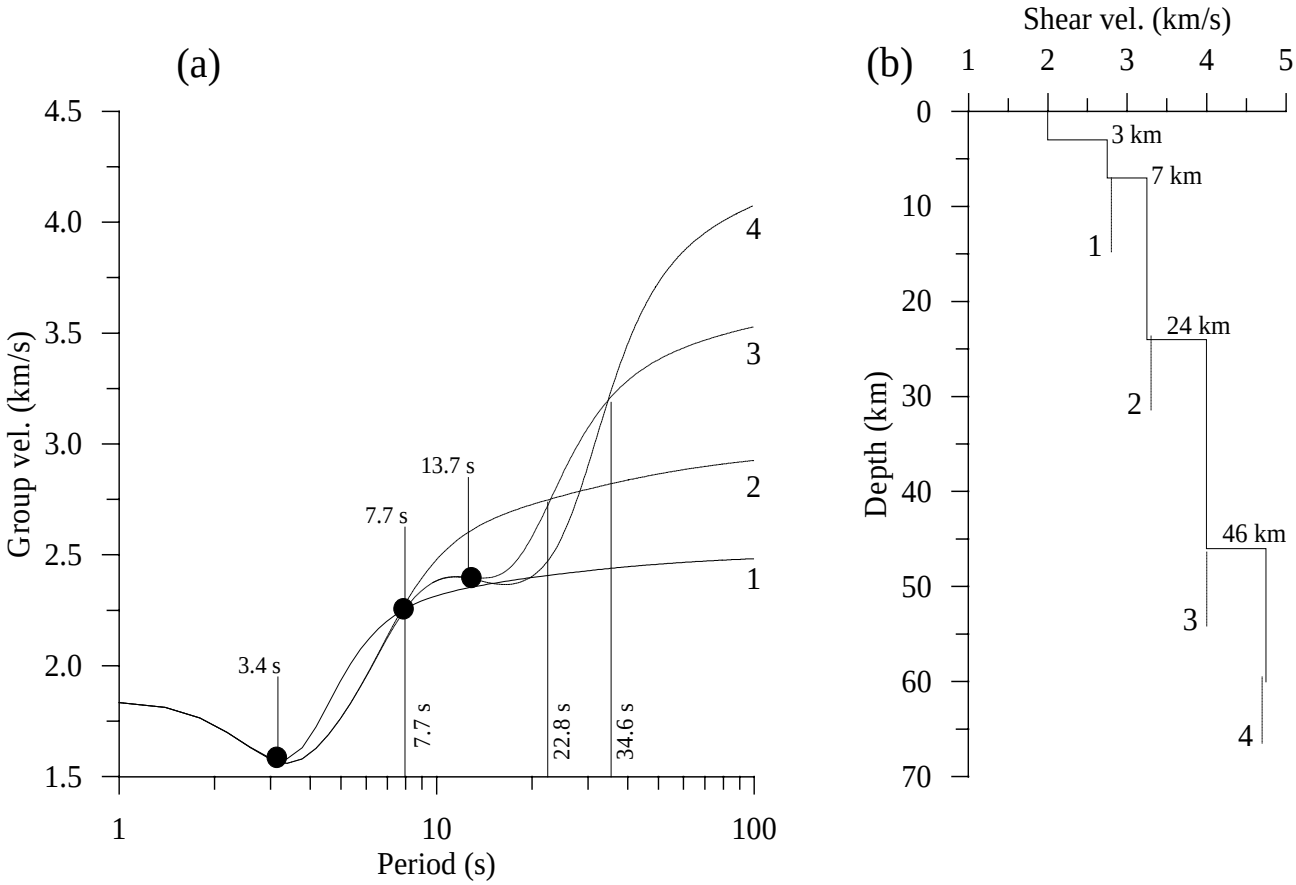

FIG. 4. Depth sensitivity of Rayleigh dispersion. The assumed model on the right represents a simplified crustal structure which is partitioned into some sub-models to demonstrate the variation of penetration depth of surface waves. On the left side four dispersion curves are shown, representing the effect of the partition above (see text for details).

The aim of this study is to explore the case of moderate size earthquakes (the magnitude may be as high as about 5.5) which can easily be approximated by a point source at equal local and regional distances. Therefore, the duration and complexity of the source time functions discussed above should be judged from this point of view. Large magnitude events will have several times longer source time functions than the ones considered in this work (see Lay and Wallace, 1995). The point source approximation, which was assumed here will fail for large events, especially when they are observed at small epicentral distances. For large events the multiple source approximation should be considered.

SINGLE-STATION INVERSION FOR GROUP VELOCITIES

We have calculated a total of 48 three component (vertical, radial and transverse) reflectivity synthetics using the parameters of four source time functions, four focal mechanisms and three crustal structures described above. This allowed us to observe the effect of changing each mode parameter on the seismic wave propagation. In Figure 3, we show two examples of such complete regional synthetic seismograms including P and S body waves and their multiples and surface waves following them. The necessary modeling parameters employed in the computations are also presented in Figure 3. It is noted that some higher mode energy arriving earlier than the fundamental mode surface wave energy is clearly evident, and needs to be removed from the fundamental mode analysis. This is achieved by the application of the multiple filter technique (Hermann, 1973) and the phase matching filter (Goforth and Herrin, 1979). The synthetics are time windowed (rectangular boxes shown in Figure 3) from 5 to 2 km/s apparent group velocity and 10 % cosine tapered at each end of the window.

The computed synthetic seismograms are treated as observed earthquake recordings and only one azimuth (65^o) of the recording station with respect to the fault plane is considered. In order to check the robustness of the results obtained different values of the station azimuth should be included in the analysis. However, we did not aim to be robust in azimuthal coverage since

two reasons kept us from doing this. First, the effective costs of calculating the reflectivity synthetics are very high in computational time and this has influenced us to narrow down the number of calculations. In addition, there are many possible choices of the fault plane orientation and the station azimuth with respect to the fault plane, so that computing the reflectivity synthetics for these variations becomes impractical. We have tried the normal mode theory (Chen, 1993) to overcome the difficulty with the computational time and are preparing the results in a compact form to be presented in a separate work. Here we focus on the effect of crustal structure, source time function and focal mechanism leaving the azimuth unchanged.

Before we attempt to analyze the inversion results, we need to perform a test for the depth resolution of group velocities. The model structure for this test is rather simple, representative of a variation of a simple crustal structure consisting of four layers over a half space (Fig. 4b). We partitioned the model from its velocity discontinuities into four sub-models including the model itself (shown by the vertical dashed lines in Figure 4b) and calculated the group velocities for each partition (Fig. 4a). For example, the second sub-model labeled as 2 consists of the first two layers and of the third layer as a half space. One observes that after each addition of a new layer to the previous model, group velocities change only for periods higher than a certain period, indicating the deep structural alteration. These group velocity changes are marked by solid circles in Figure 4a and the separation between the various curves increases with the period. Let us, for example, examine the difference between cases 3 and 4. As indicated, until the 13.7 s period there is no difference between group velocities 3 and 4, which means that surface waves below the 13.7 s period are not sensitive to structure below a depth of 24 km. As the period increases towards 34.6 s, a deviation between group velocities 3 and 4 occurs, but the deviation is not so distinct, since group velocities in that period range are weakly sensitive to the structure below a depth of 24 km. Beyond the 34.6 s period the surface waves become increasingly sensitive to the deeper structure, even below a depth of 46 km. The results of this test can be used as a rough measure of the period sensitivity with depth.

As mentioned earlier, we have included the effect of anisotropic wave propagation in the inversions. The propagation media is characterized as transversely isotropic with a vertical symmetry axis and the inversion is performed for six parameters. The necessary mathematical formulation for transverse isotropy is given in Takeuchi and Saito (1972). The necessary model parameters are the ρ (density), PV and SV (P and S velocity for vertical transmission), PH and SH (P and S velocity for horizontal transmission) and η (parameter controlling the velocity change with an angle of incidence). We employed the least square algorithm of Tarantola (1987) which has been successfully applied to wave propagation problems (Hadiouche and Zürn, 1992). The properties of a transverse isotropic media is taken from Anderson (1993).

Although the test model structures shown in Figures 1a-c are actually isotropic, we performed an anisotropic inversion, for several reasons. Initially, it should be mentioned that we did not isolate the effect of the initial phase at the source from the synthetics. In such a case, it is reasonable to suspect that this remnant phase may result in an erroneous inversion of velocities. If the observed group velocities after a multiple filter analysis reflect the true seismic propagation, then inversion will truly produce an isotropic velocity depth profile. Moreover, although the medium is isotropic, it is possible that the inversion may falsely show anisotropy because of the effect of the initial phase at the source. This is indeed the case and we show how severe this falsification could be.

The analysis revealed that inverted group velocities were slightly sensitive to a change in the source time function from one type to the other in Figure 2, hence we only present results for the source time function shown in Figure 2a. It can be seen that this source time function has the most rapid variation with frequency and is thus expected to have the largest effect on the actual group velocities. In the following, we present the group velocity inversion results for each model shown in Figures 1a-c. In the presentation of results, the maximum period is set to be 40 s since, at a 350 km epicentral distance, this is the highest observable surface wave period. The group velocities are retrieved from the synthetic seismograms with an application of a multiple filter (Hermann, 1973) and a phase matching filter (Goforth and Herrin, 1979) techniques along with a time variable filtering (Mindevalli, 1988).

Model 1

The inversion results for this model are shown in Figure 5. The figure consists of four inversions performed with strike slip, dip slip, normal and reverse oblique faulting, respectively. Here the inverted velocity depth profile should be compared to the true velocities given in Figure 1a. Although no correction for the initial phase shift at the source is performed, the overall picture of the inverted velocities with depth shows a reasonable match to the true velocities, except within the 50-65 km depth range where the true velocity profile does not have the low velocity zone, such as the one featured in the inversion results. One should

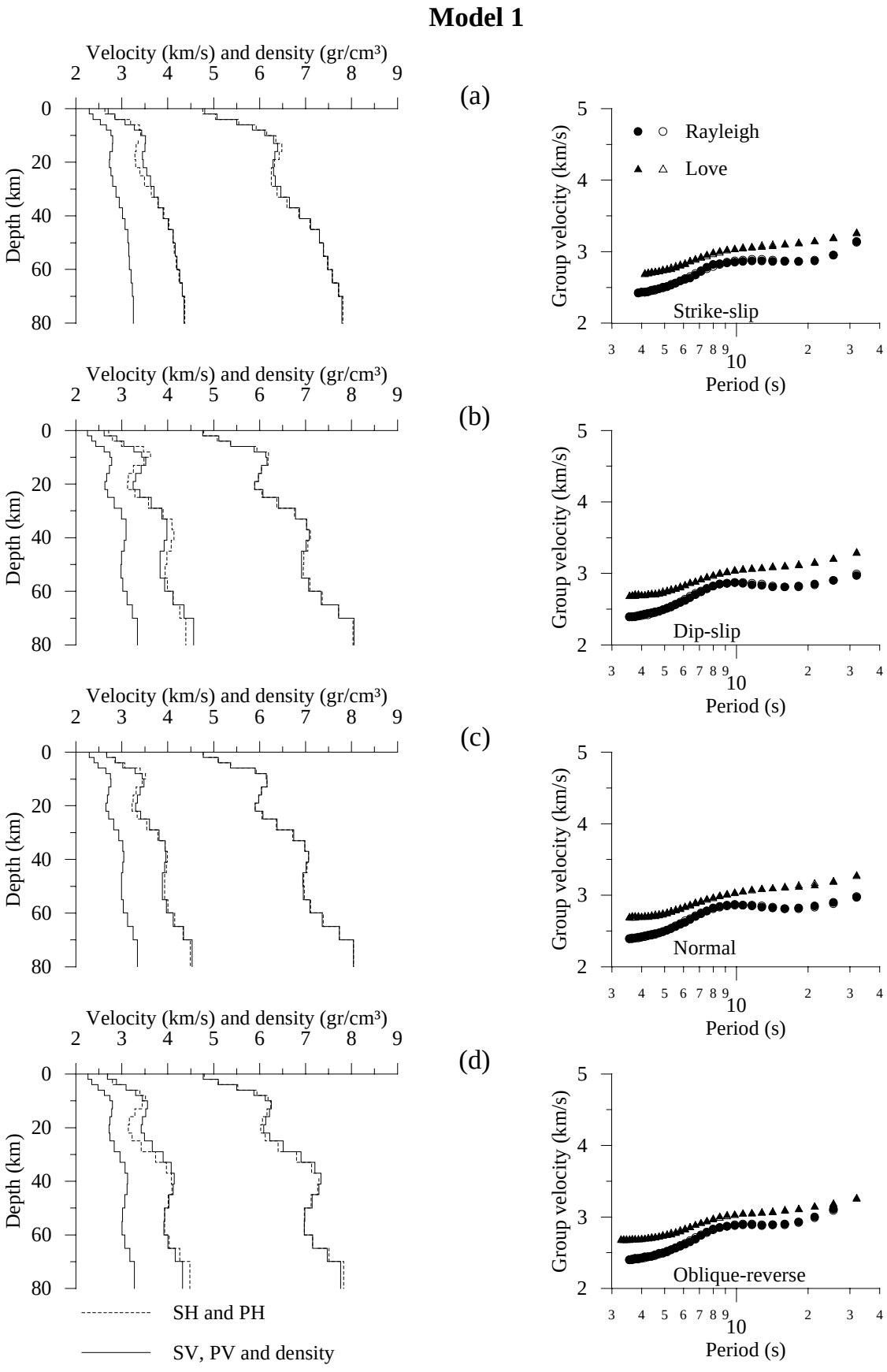

FIG. 5. Group velocity inversion results for Model 1. The inversion is performed by employing four different focal mechanisms as indicated and anisotropy is included in the inversion process (see text for more explanations).

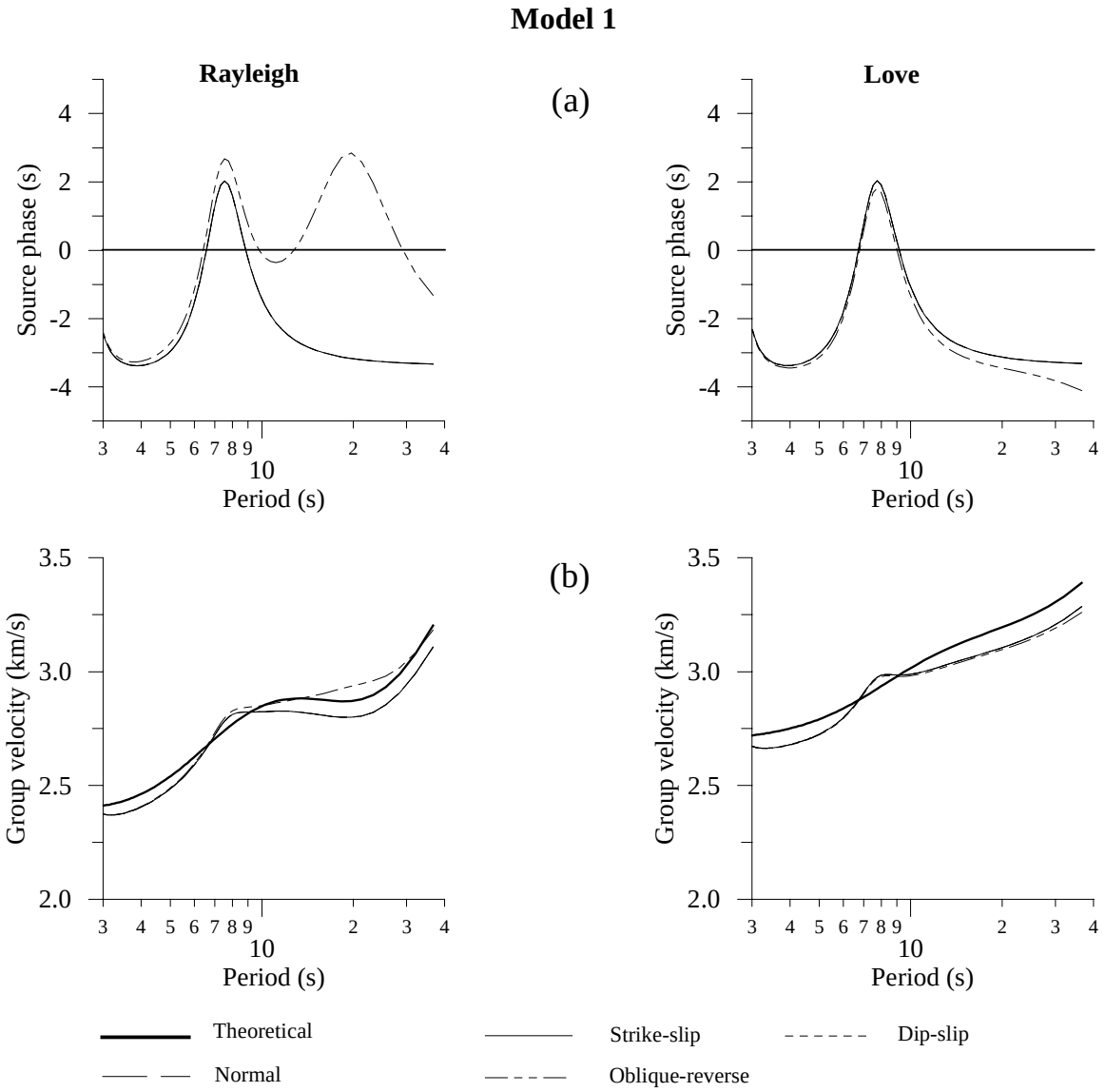

FIG. 6. The effect of the source phase function on group velocities in Model 1 is illustrated. (a) Rayleigh and Love wave source phase functions, (b) Theoretical group velocities and the group velocities modified by the source phase at a 350 km epicentral distance (see text for more explanations).

compare the dispersion curves on the right in Figure 5, retrieved from the synthetics, to the true dispersion curves on the right in Figure 1a. It can be seen that the retrieved dispersion curves are systematically lower than the actual ones and this deviation gradually increases with increasing the period. The curvature in group velocities at around the 9 s period is falsely exaggerated by the non-corrected source phase effect. Group velocities at around the 40 s period should converge to about 3.5 km/s (Fig. 1a) for both Rayleigh and Love waves, but they reach as high as only up to about 3.25 km/s and even up to a lower value for Rayleigh waves (on the left in Figueres 5a-d). This behavior of group velocities for long periods indeed lowers the inverted velocities at deeper levels. The inverted structure with a strike-slip mechanism is the most correct one as compared with the other fault mechanisms employed (see Figs. 1b-c).

It should be noted that the inversion shows some anisotropy at depths from about 10 to 30 km, although the opposite should be true. Here the anisotropy is revealed by the separation between SH (dashed line) and SV (solid line) velocities. This false identification of anisotropy is observed for all the selected mechanisms, but is less significant in the case of normal faulting. This situation arises mainly because of the Rayleigh and Love wave incompatibility (see Mitchell, 1984) resulting from the source phase shift effect.

Up to this point we have analyzed the situation with no knowledge of the source phase spectrum. In Figure 6, we show the Rayleigh and Love wave fundamental mode phase spectra for each case in Figure 5. The

necessary mathematical formulation is adapted from Aki and Richards (1980). The source phase functions (Fig. 6a) and theoretical and source phase distorted group velocities are also shown (Fig. 6b). One should note that all the selected fault mechanisms (except for oblique-reverse faulting) are extreme (degenerate) cases for which the source phase does not change with frequency for a given azimuth (see Levshin *et al*., 1999). Thus, for the degenerative mechanisms the source phase shift originates from the effect of the source time function alone, as can be seen from a comparison between Figure 2a and Figure 6a. The source phase related to the oblique-reverse faulting differs from the others, especially high periods and significantly for Rayleigh waves. We show in Figure 6b how much the group velocities are scattered away from the true velocities after the effect of the source phase shift. The scatter is significant for both Rayleigh and Loves and Figure 5 shows how this scatter alters the inversion results.

It is noted that in Figures 6a and 6b, the source phase functions for strike slip, dip slip and normal faulting are all the same and the curves drawn for these rupture mechanisms by different line patterns all coincide with each other, except for oblique-reverse faulting.

Model 2

The inversion results for this model are illustrated in Figure 7. Here quite satisfactory results are obtained compared to the previous one. The velocity depth profile in Model 2 hosts basically three features: a low crustal thickness, an almost constant positive velocity gradient in the crust and a low velocity zone below the crust. It can be seen that these features are all successfully retrieved in the inversion process. Note that the difference between the current and the previous inversion process is only a change in the model parameters, but the source time function and the focal mechanisms were not changed. This reveals how effectively elastic parameters around the source region can alter the inversion results. On the other hand, we observe some false identification of anisotropic propagation, which is shown by the deviation between the solid (PV and SV) and dashed (PH and SH) lines, although the opposite should be true. This false identification is more important for S waves than for P waves, and results from the fact that the initial source phase is not corrected to a zero phase, i.e. the aforementioned Rayleigh and Love incompatibility.

In Figure 8, the initial source phase spectra and the scatter of group velocities for this model is presented. We can see that the scatter in the group velocities because of the source phase shift is significant, similar to the case shown in the previous model. However, the structure is retrieved rather well, unlike the former case. It is again noted that, in Figures 8a and 8b, the source phase functions for strike slip, dip slip and normal faulting are all the same and the curves drawn for these rupture mechanisms by different line patterns all coincide, except for oblique-reverse faulting.

Model 3

The inversion results for this model are illustrated in Figure 9. Here we can observe better the decisive effect of the elastic parameters in the source region. The model hosts rather unusual features and is inverted poorly at especially deeper levels. The structure is resolved satisfactorily up to a depth of 25 km, but the low velocity zone originally configured in the lower crust is not resolved after the inversion process. Although the true crustal thickness of this model is 50 km, it is estimated to be deeper (around 60 km) from the inversion results. The anisotropic falsification mentioned above is also important for Model 3 and happens mainly within the depth range 15-30 km.

The situation described above can be better understood by the source phase spectrum plots in Figure 10. Again the scatter in the group velocities is as significant as in the former two cases. But in this model it is so effective that the inverted structure at deep levels lacks some resolution, in a way that below a depth of 25 km the inverted velocities change smoothly (Figs. 9a-d) in contradiction to the assumed model (Fig. 1c). This occurs because the source phase affected group velocities particularly for long periods as retrieved from the synthetics lose those important features necessary to resolve the deep low velocity zone in the model. It is noted that, in Figures 10a and 10b, the source phase functions for strike slip, dip slip and normal faulting are all the same and the curves drawn for these rupture mechanisms by different line patterns all coincide with each other, except for oblique-reverse faulting.

A CASE STUDY OF AN EARTHQUAKE

We selected an earthquake recording in order to demonstrate the power of single station method. Table 2 lists the source parameters of the selected event, which is geographically located near city of Corum, Turkey. This event was recorded at seismic station TBZ, Trabzon, Turkey (located at 39.77N and 40.99E) equipped with a three component digital broad-band sensor. The seismometer is a Guralp CMG-40 with a flat velocity response between 0.05 and 20 Hz. We performed a group velocity inversion for the vertical

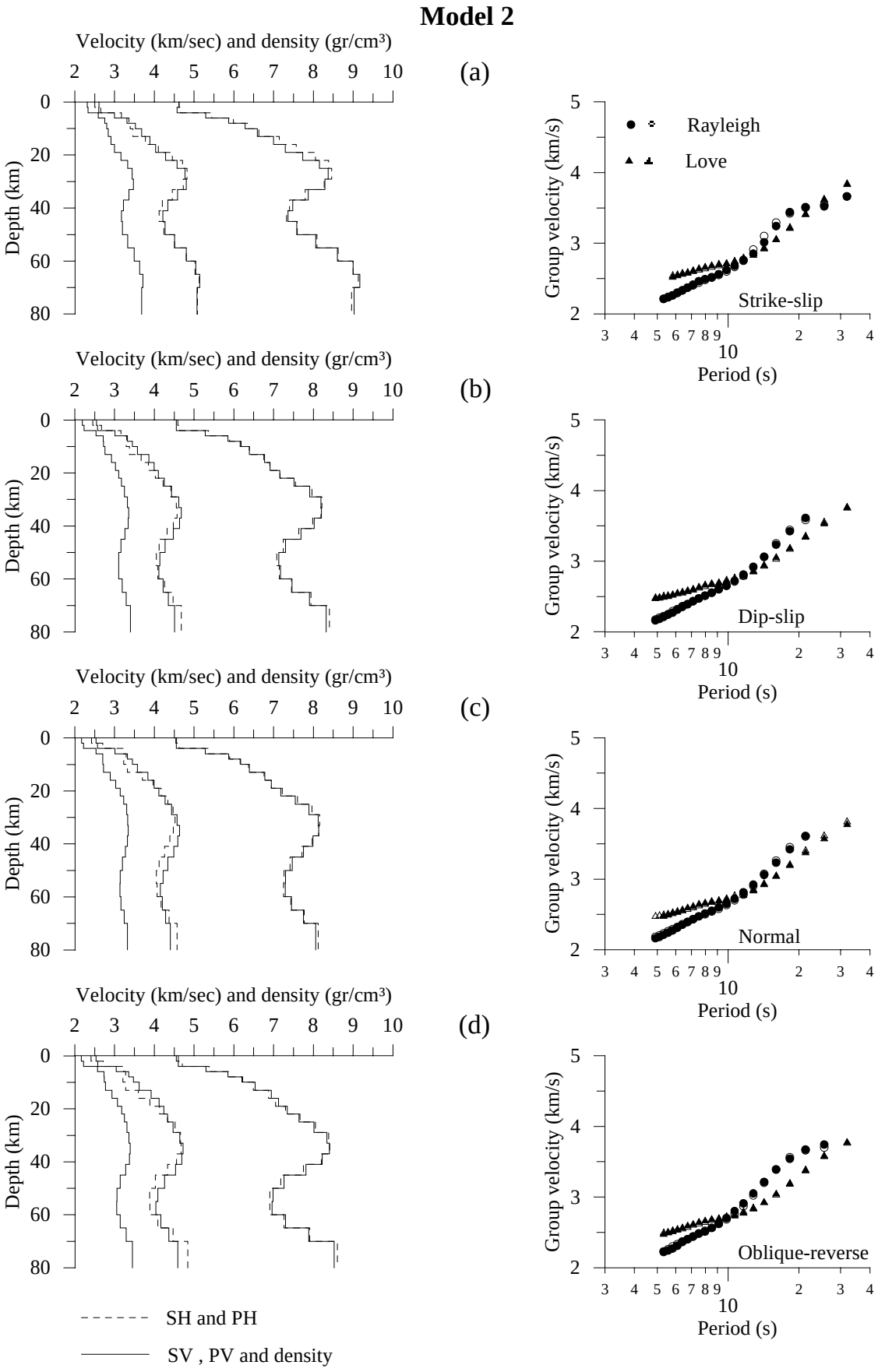

FIG. 7. Group velocity inversion results for Model 2. The inversion is performed by employing four different focal mechanisms as indicated and anisotropy is included in the inversion process (see text for more explanations).

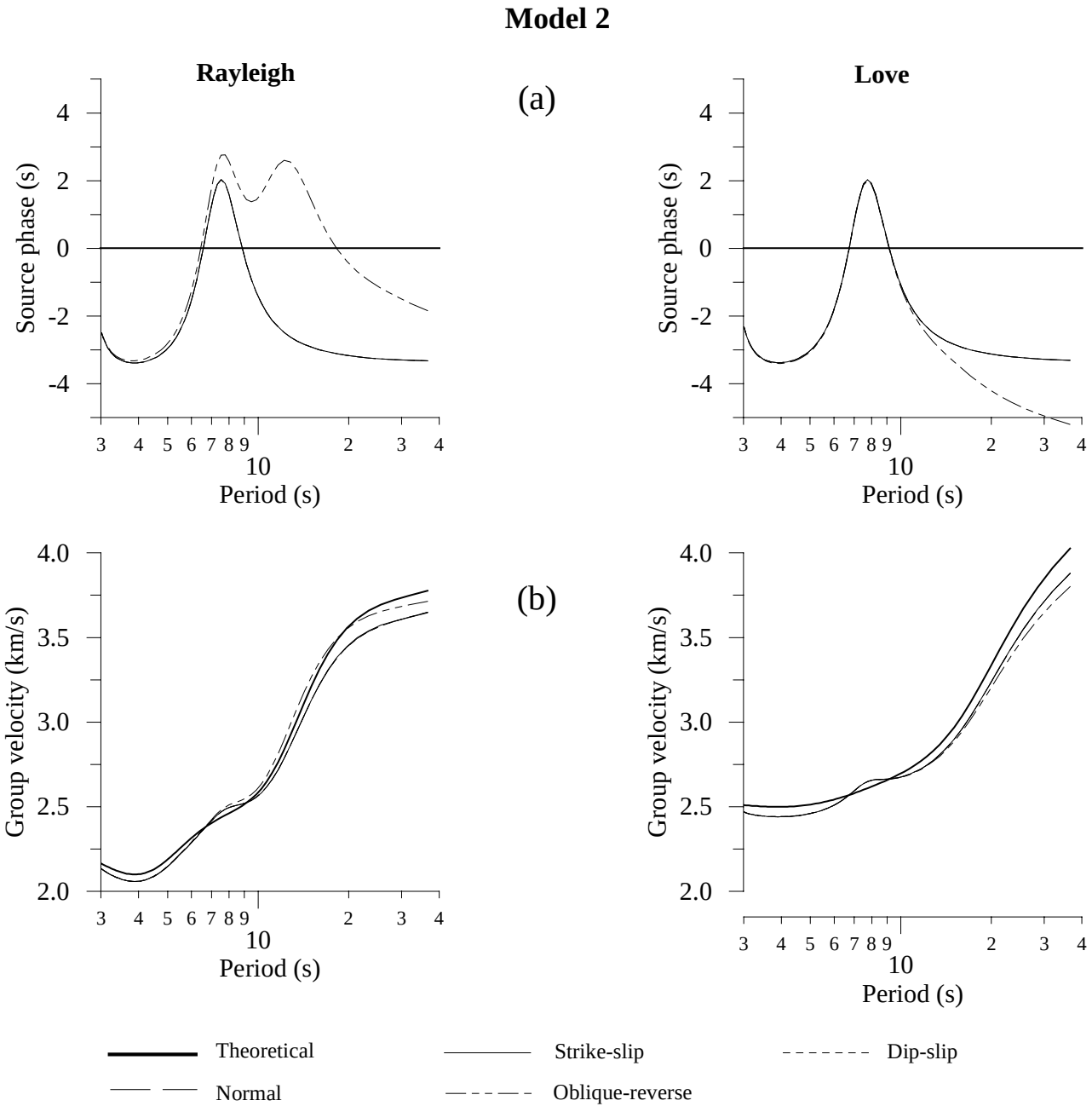

FIG. 8. The effect of the source phase function on group velocities in Model 2 is illustrated. (a) Rayleigh and Love wave source phase functions, (b) Theoretical group velocities and the group velocities modified by the source phase at 350 km epicentral distance (see text for more explanations).

component fundamental mode Rayleigh and the transverse component fundamental mode Love waves. The inversion was performed for both Rayleigh and Love waves, simultaneously. Instrumentally corrected seismograms were time windowed with the apparent group velocity between 5 and 2 km/s. During the inversion we followed the procedure described by Dean and Keller (1991). After processing the fundamental mode by this procedure, the effect of noise, multiple arrivals and higher mode interactions were significantly reduced.

The observed group velocity curves and the corresponding inversion results are both depicted in Figure 11. The source effect was not taken into account for dispersion inversion. For this event, the observable periods after multiple filter analysis go as high as 30 s, but we allowed the maximum period in the inversion to be around 20 s, in order to reduce the effect of the source phase shift. The inversion is performed both for isotropic and transversely isotropic models, in order to detect a possible anisotropic wave propagation for the path which this earthquake traverses. If the medium is

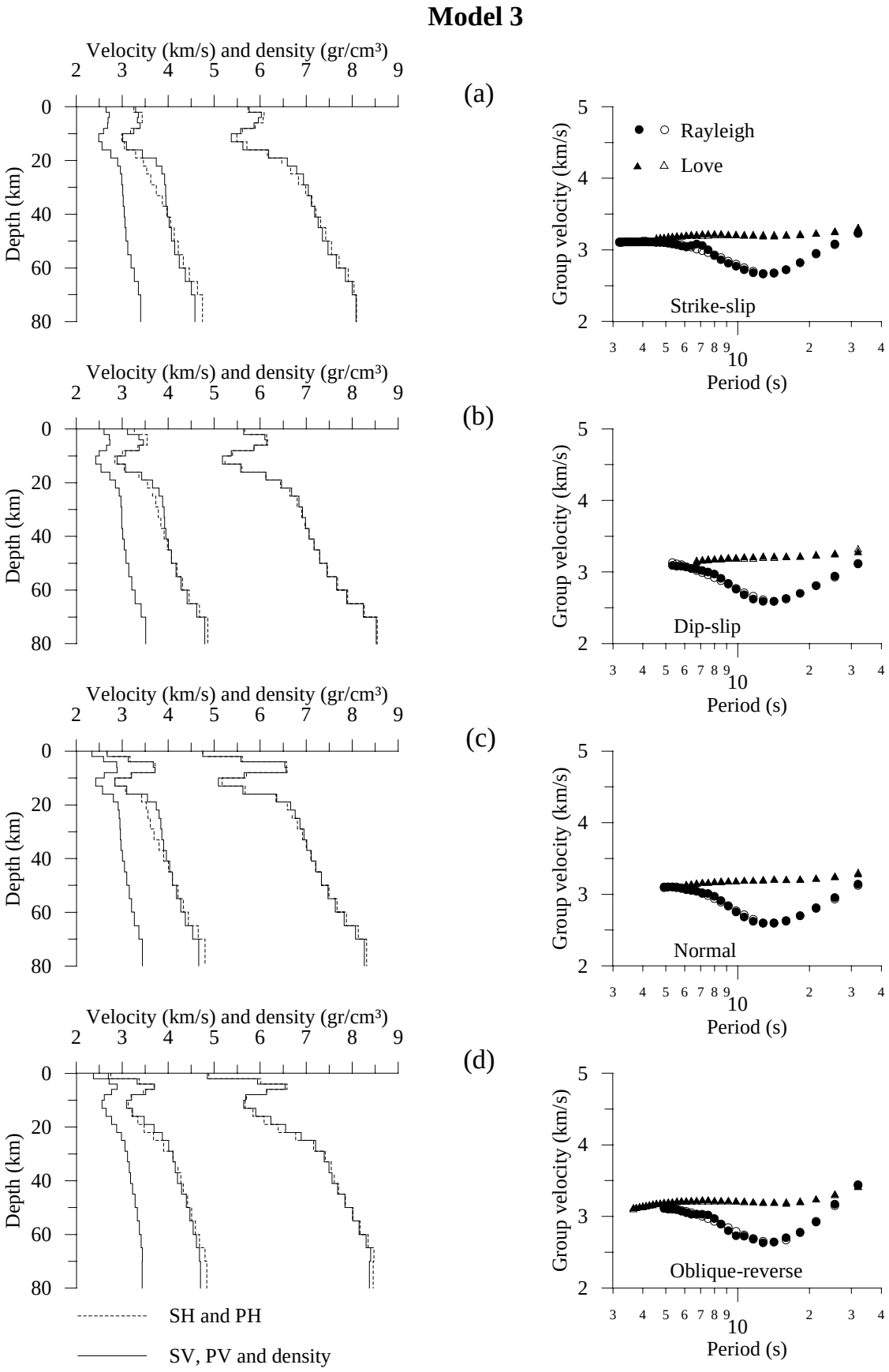

FIG. 9. Group velocity inversion results for Model 3. The inversion is performed by employing four different focal mechanisms as indicated and anisotropy is included in the inversion process (see text for more explanations).

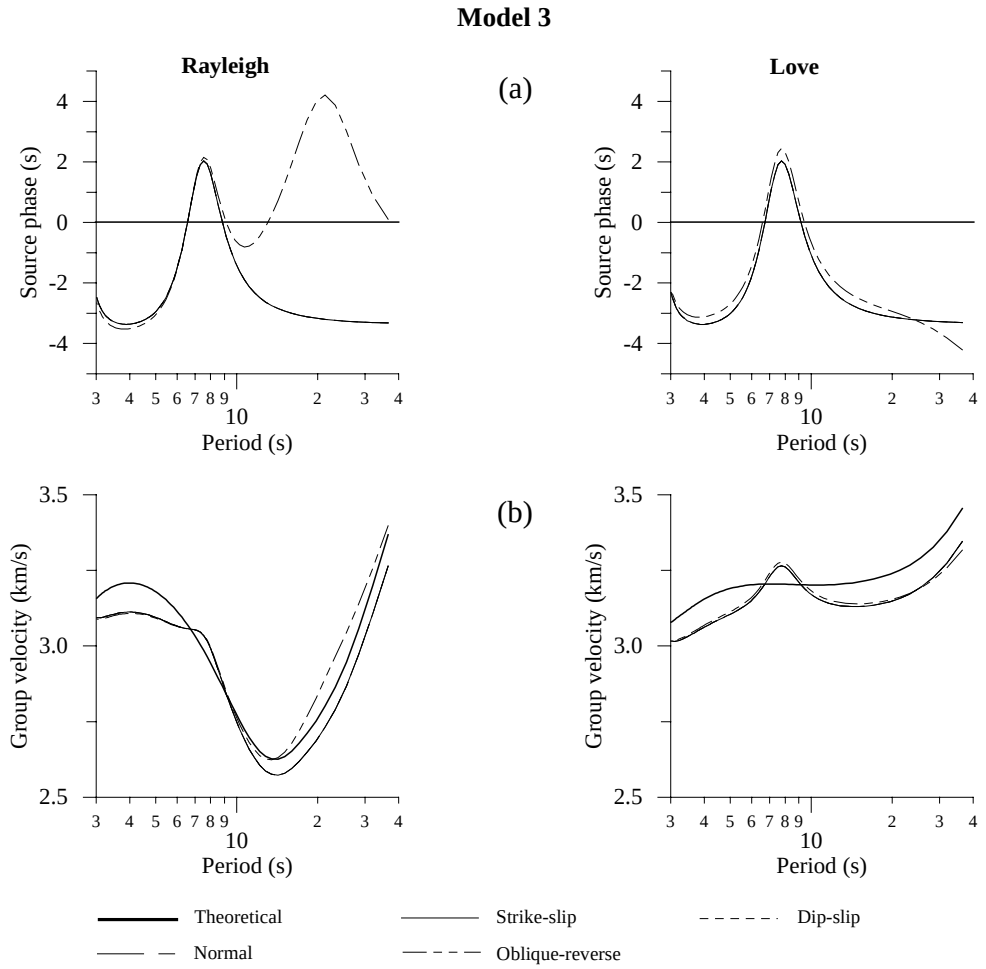

FIG. 10. The effect of the source phase function on group velocities in Model 3 is illustrated. (a) Rayleigh and Love wave source phase functions, (b) Theoretical group velocities and the group velocities modified by the source phase at a 350 km epicentral distance (see text for more explanations).

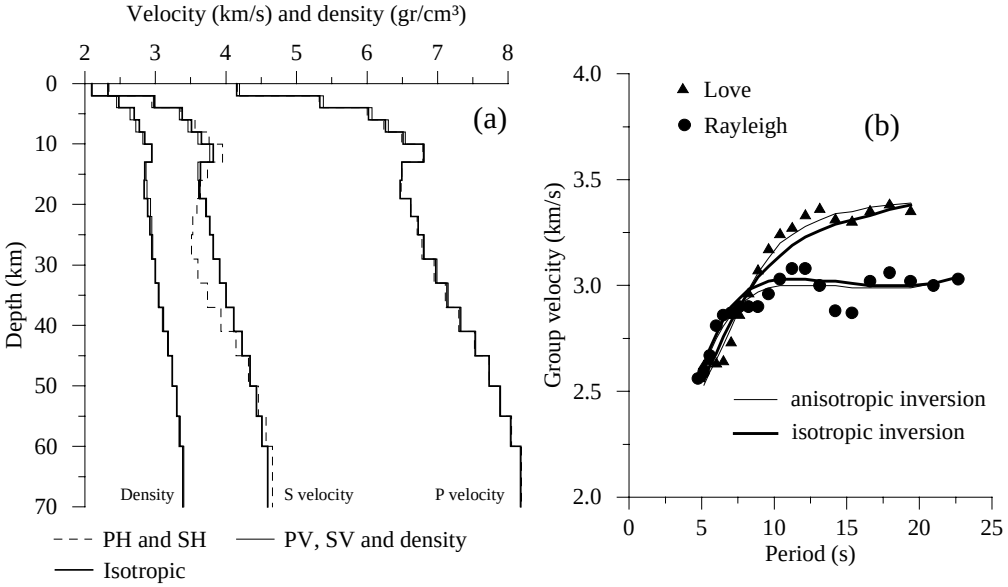

FIG. 11. Group velocity inversion results for the earthquake listed in Table 2. The inversion is performed for both isotropic and transversely isotropic media (the isotropic results are depicted by a thicker line). The difference between SH and SV velocities in the transversely isotropic solution within the depth range of 20-40 km is particularly important. (see text for more explanations).

Table 2. Parameters of the earthquake used for a case study.

Date	Origin Time (UTC)	Lat. (N^o)	Long. (E^o)	Azimuth (deg.)	Distance (km)	Depth (km)	Magn. (m_b)
08/14/1996	01:55:02.7	40.75	35.34	85	374	17	5.6

Parameters taken from KOERI (Kandilli Observatory of Earthquake Research Institute, Turkey)

isotropic, then both isotropic and transversely isotropic inversions should produce similar results. In Figure 11, the isotropic inversion results are displayed by a thicker line. We observe that the isotropic and anisotropic inversion for Rayleigh waves are not very different from each other (Fig. 11b). However, this difference becomes more pronounced for Love waves particularly for large periods. The previous analysis shows that when no correction is applied for the source phase shift, it may lead one to a false identification of an isotropic medium as anisotropic.

In order to check the results of Figure 11 more properly, we also performed synthetic seismogram computations. The observed fundamental mode Rayleigh and Love wave signals were isolated from the recordings by phase matching filter (Goforth and Herrin, 1979) and time variable filter (Mindevalli, 1988) techniques, as utilized by Hermann (1987) in Computer Programs in Seismology package. The focal mechanism solution for the current earthquake is reported by NEIC to have a strike = 119^o, a dip = 84^o and a rake = 172^o, which is approximately a right lateral strike-slip mechanism. After some trial and error, our synthetic seismogram analysis showed that the strike direction should be changed to around 145^o. This change helped us to control more properly the energy distribution

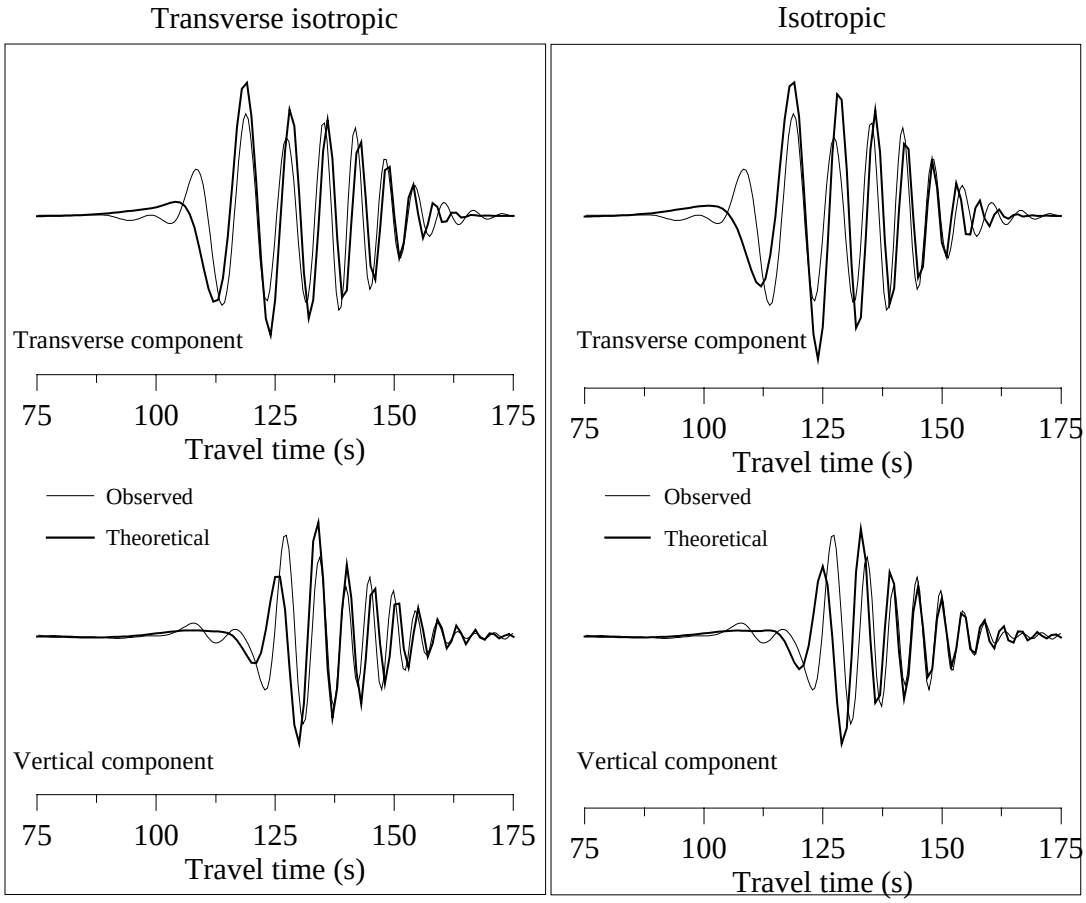

FIG. 12. Vertical component Rayleigh and transverse component Love wave fundamental mode traces for the earthquake listed in Table 2. Synthetic modeling is performed both for isotropic and transversely isotropic media. The synthetic traces are imposed on the observed traces by a thicker line (see text for more explanations).

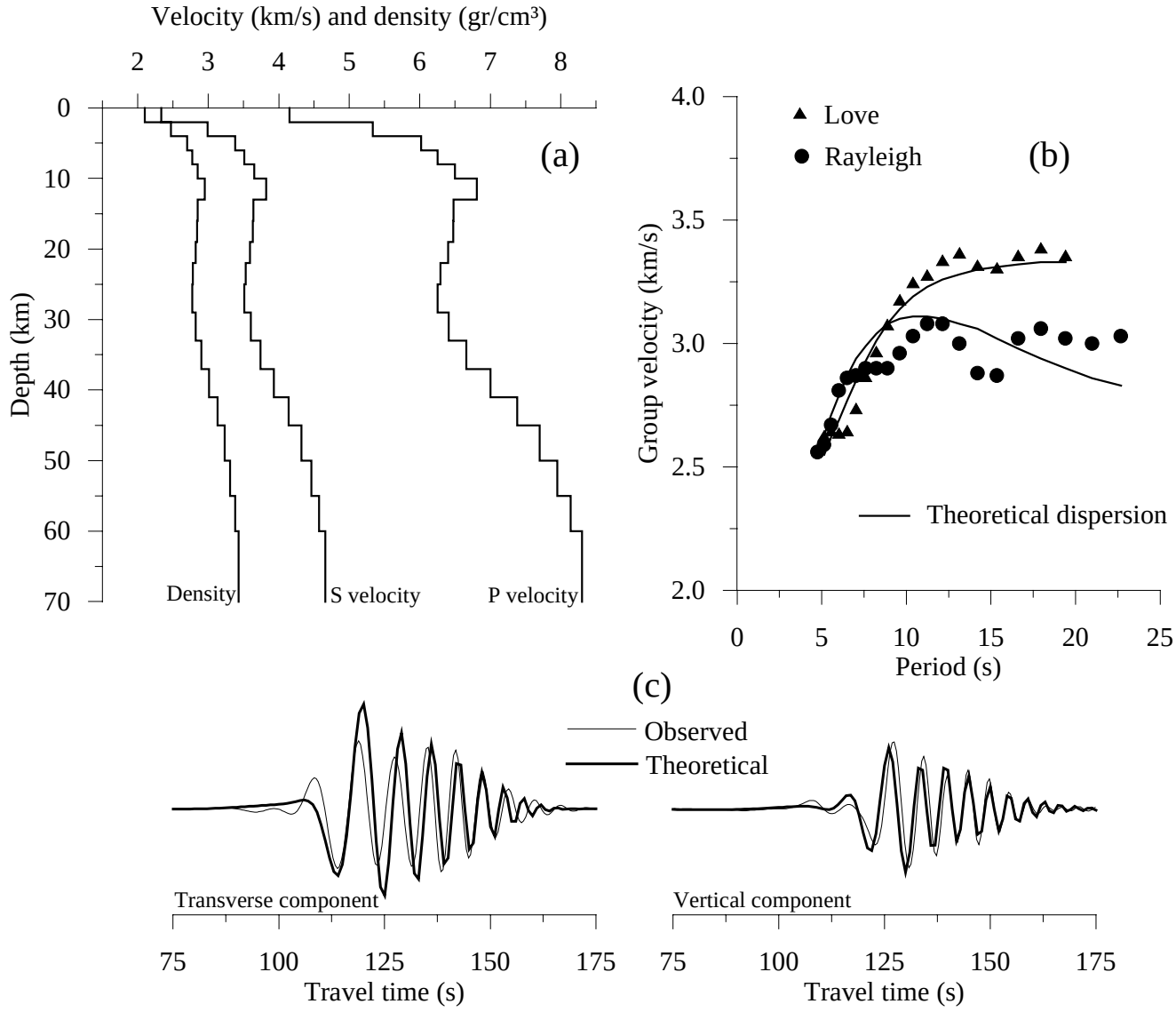

FIG. 13. Isotropic modeling results for the earthquake in Table 2. a) The isotropic crustal structure. b) The observed and theoretical dispersion curves. c) The match between observed and theoretical signals. The observed signals are better explained by the proposed isotropic model structure. Note that the observed dispersion is matched poorly by the theoretical one.

between the Rayleigh and Love waves at the source. We were able to simulate the source moment rate function by a simple triangular pulse with a pulse duration of around 5 s. The match between the computed (thick line) and the observed fundamental surface wave signals, free of instrument response, are shown in Figure 12. Synthetic signals are produced for both isotropic and anisotropic inversion structures in Figure 11a. It can be noted that the overall match for the anisotropic case is slightly better as compared to the isotropic case.

It can also be noted that both the anisotropic and the isotropic synthetic signals fail to match the observed particularly high apparent group velocities. This immediately suggests the adjustment of velocities to some lower values at middle crustal levels. The isotropic crustal structure as shown in Figure 13a produces the synthetic signals matching better the observed ones (Fig. 13c). However, the match between the observed dispersion and the theoretical one is poor, as compared to the case given in Figure 11b, particularly for Rayleigh waves (Fig. 13b). This occurs because the observed group velocities are influenced by the source phase shift and obviously the Rayleigh waves are more influenced. The Rayleigh and Love wave incompatibility mentioned above can be better seen in this example and causes the false identification of an isotropic structure as an anisotropic (Fig. 11a).

DISCUSSION AND CONCLUSION

We have shown that, in case it is not possible to perform a two-station analysis for the data, a single-station method can be used for local and regional earthquake recordings. However, in this case, it has been shown that under certain conditions seismic velocities particularly at deep structural levels, may not be resolved satisfactorily. We suggest that, before going to synthetic modeling, one should consider inverting the surface waves for estimating the focal mechanism. This kind of inversion is frequently applied for far-field, such as upper-mantle recordings since they are relatively more insensitive to the source phase shift (Giardini *et al*., 1993, Jimenez *et al*., 1989, Mendiguren, 1977). Ceratainly, the estimated focal mechanism at local and regional distances determined by this method may have some bias to a certain degree. Our preliminary work on this subject has yielded some promising results that we will incorporate in a subsequent work.

The crustal studies (particularly focusing on anisotropy) are important in forming better geodynamical models of the crustal structure. With sufficient local and regional seismological data available, this task can be achieved by some careful and skilled analysis, and the source phase effect should be included in the analysis scheme. This kind of work can be very helpful in resolving conflicts, for example, in surface wave tomography of regional surface recordings.

ACKNOWLEDGMENTS

We would like to thank the anonymous reviewers for the critical reviewing of the manuscript.

REFERENCES

Aki, K. and Richards, P. G., 1980. Quantitative seismology: Theory and methods: W. H. Freeman and Company, San Francisco, 259-333.

Ammon, C. J., Randall, G. E. and Zandt, G., 1990. On the nonuniqueness of receiver function inversions: Journal of Geophysical Research, **95**, 15303-15318.

Anderson, D. L., 1989. Theory of the earth: Blackwell Scientific Publications, Brookline Village, MA, 303-333.

Barka, A. A. and Kadinsky-Cade, K., 1988. Strike-slip fault geometry in Turkey and its influence on earthquake activity: Tectonics, **7**, 663-684.

Chen, X., 1993. A systematic and efficient method of computing normal modes for multilayered half-space: Geophys. J. Int., **115**, 391-409.

Crampin, S. and Booth, D. C., 1985. Shear-wave polarizations near the North Anatolian fault-II. Interpretation in terms of crack-induced anisotropy: Geophys. J. R. Astr. Soc., **83**, 75-92.

Dean, E. A. and Keller, G. R., 1991. Interactive processing to obtain interstation surface-wave dispersion: Bull. Seism. Soc. Am., **81**, 931-947.

Dziewonski, A. M. and Hales, A. L., 1972. Numerical analysis of dispersed seismic waves: in Methods in computational Physics: Bolt, B. A. (ed.), Academic Press, New York, **11**, 39-84.

Frez, J. and Schwab, F., 1976. Structural dependence of the apparent initial phase of Rayleigh waves: Geophys. J. R. Astr. Soc., **44**, 311-331.

Giardini, D., Boschi, E. and Palombo, B., 1993. Moment tensor inversion from Mednet data (2) regional earthquakes of the Mediterranean: Geophy. Res. Let., **20**, 273-276.

Goforth, T. and Herrin, E., 1979. Phase-matched filters: application to the study of Love waves: Bull. Seism. Soc. Am., **69**, 27-44.

Hadiouche, O. and Zürn, W., 1992. On the structure of the crust and upper mantle beneath the Afro-Arabian region from surface wave dispersion: Tectonophysics, **209**, 179-196.

Hermann, R. B., 1973. Some aspects of band-pass filtering of surface waves: Bull. Seism. Soc. Am., **63**, 663-671.

Hermann, R. B., 1987. Computer programs in seismology, user's manual, vol. IV, St. Louis University, Missouri.

Jimenez, E., Cara, M. and Rouland, D., 1989. Focal mechanisms of moderate-size earthquakes from the analysis of single-station three-component surface-wave records: Bull. Seism. Soc. Am., **79**, 955-972.

Lay, T. and Wallace, T. C., 1995. Modern global seismology: Academic Press. Inc., San Diego, 397-433.

Levshin, A. L., Ritzwoller, M. H. and Resovsky, J. S., 1999. Source effects on surface wave group travel times and group velocity maps: Phys. Earth Planet. Inter., **115**, 293-312.

Maslova, S. I. and Obolentseva, I. R., 1984. An anisotropic model of the earth' s crust in the Baikal rift zone: Geophys. J. R. Astr. Soc., **76**, 227-232.

Mendiguren, J. A., 1977. Inversion of surface wave data in source mechanism studies: J. Geophys. Res., **82**, 889-894.

Mindevalli, O. Y., 1988. Crust and upper mantle structure of Turkey and the Indian sub-continent surface wave studies: Ph.D. thesis, Univ. of Saint Louis.

Mindevalli, O. Y. and Mitchell, B. J., 1989. Crustal structure and possible anisotropy in Turkey from seismic surface wave dispersion: Geophys. J. Int., **98**, 93-106.

Mitchell, B. J., 1984. On the inversion of Love and Rayleigh wave dispersion and implications for earth structure and anisotropy: Geophys. J. R. Astr. Soc., **76**, 233-241.

Mokhtar, T. A. and Al-Saeed, M. M., 1994. Shear wave velocity structures of the Arabian Peninsula: Tectonophysics, **230**, 105-125.

Müller, G., 1985. The reflectivity method: a tutorial: J. Geophys., **58**, 153-174.

Navarro, M., Corchete, V., Badal, J., Canas, J. A., Pujades, L. and Vidal, F., 1997. Inversion of Rg waveforms recorded in southern Spain: Bull. Seism. Soc. Am., **87**, 847-865.

Takeuchi, H. and Saito, M., 1972. Seismic surface waves: in Methods in computational Physics: Bolt, B. A. (ed.), Academic Press, New York, **11**, 217-294.

Tarantola, A., 1987. The least-squares criterion: in Inverse problem theory: Elsevier Science Company Inc., New York, 187-255.